Applied Surface Science 498 (2019) 143831

Contents lists available at ScienceDirect

Applied Surface Science

journal homepage: www.elsevier.com/locate/apsusc

Full length article

Thermally induced atomic and electronic structure evolution in nanostructured carbon film by in situ TEM/EELS analysis

Nan Jian[a,b], Peidong Xue[a], Dongfeng Diao[a,b,*]

[a] Institute of Nanosurface Science and Engineering, Shenzhen University, Shenzhen 518060, China
[b] Electron Microscopy Center, Shenzhen University, Shenzhen 518060, China

ARTICLE INFO

Keywords:
Carbon film
Atomic structure
In-situ TEM
In-situ EELS
ECR

ABSTRACT

The atomic and electronic structures of nanostructured carbon film are of fundamental importance due to their dominant role in carbon films' physical, chemical and mechanical properties. Here, we reported thermally induced atomic and electronic structure evolution of nanostructured carbon film by in-situ transmission electron microscopy (TEM) and electron energy loss spectroscopy (EELS). Two nanostructured carbon films were synthesized by electron cyclotron resonance (ECR) plasma sputtering under ion and electron irradiation, respectively. We observed that even though the two carbon films had similar initial sp2/sp3 hybridization ratio, they exhibited very different performance during the same heating process. The electron irradiated film only had a relative slight clustering of sp2 carbon crystallites and almost maintained its sp2/sp3 ratio till 1000 °C; while the ion irradiated film had a significant sp2 crystallites clustering, started its sp3-to-sp2 conversion from 200 °C and almost completed at 400 °C. Argon signal was only found in the ion irradiated carbon film and its content reduced simultaneously with the sp3-to-sp2 conversion process. We suggest that the heated argon trapped inside the carbon film were responsible for triggering the sp3-to-sp2 conversion. The result will guide the future application of the nanostructured carbon film in the proper operation temperature range and help to choose appropriate irradiation method for thin film surface modification.

1. Introduction

Carbon based films have drawn tremendous attentions due to their unique physical, chemical and mechanical properties combine with the good economic efficiency and eco-friendly character, leading to a wide range of applications from daily used razor blade to spacecraft [1–10]. In all kinds of different carbon based film, the nanostructured carbon films deposited by ion or electron irradiated ECR sputtering method are of great interest due to its special structure of controllable nanosize graphene sheets embedded in the amorphous carbon matrix with an orientation vertical to the film [11–15]. This unique structure provides fast electron transport channel, lubricant graphene-graphene interface, hard amorphous matrix and abundant graphene edge defect, giving the carbon film excellent properties in magnetoelectricity, piezoelectricity, mechanical tribology and catalysis activity, showing the great promise for applications including magnetic sensing, piezo sensing, lubricant coating and electrochemical catalysis [16–23]. During the graphene sheets embedded carbon film deposition, the size and density of graphene sheets embedded can be modified effectively under ether original ion beam irradiation (most are Ar^+) or newly developed electron beam irradiation by tuning the beam irradiation energy and density. These two modification methods have different principles and leave different residuals (trapped electrons and argon atoms) in the carbon films [11,13–15]. In the electron beam irradiated carbon film, some irradiation electrons were trapped in the quantum well in the graphene edge defect, induce the magnetics property of the carbon film [21,24,25]. In the ion irradiated sample, a considerable amount of argon atoms were trapped inside the carbon film, but their existence and influence have long been neglected due to the inert nature of argon.

The influence of the high temperature environment on the carbon film has both fundamental and practical importance. Numerous studies on the influence of high temperature on carbon films' structures and properties have been performed [7,26–36]. Generally, the previous studies suggest that the high temperature causes the transformation of sp3 hybridization to sp2 and the clustering of sp2 bonded atoms, which changes the corresponding properties of the carbon films. For the hydrogenated amorphous carbon (a-C:H) film, the break of weak C—H bond is believed to limit its high temperature stability [26,27,35,36]. Li et al. reported the annealing effect on the structure and properties of a-C:H films, the diffusion of hydrogen and sp3-to-sp2 conversion occurred

* Corresponding author at: Institute of Nanosurface Science and Engineering, Shenzhen University, Shenzhen 518060, China.
E-mail address: dfdiao@szu.edu.cn (D. Diao).

https://doi.org/10.1016/j.apsusc.2019.143831
Received 8 April 2019; Received in revised form 15 August 2019; Accepted 29 August 2019
Available online 30 August 2019
0169-4332/

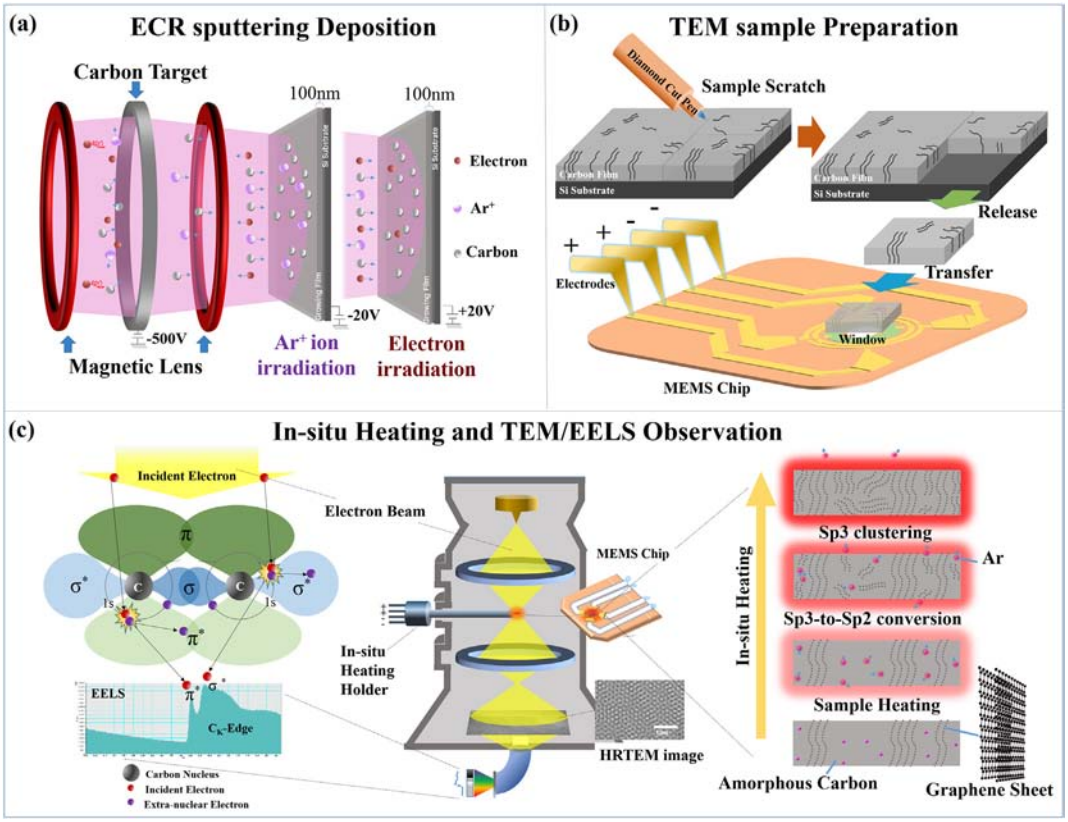

Fig. 1. Schematic of (a) ECR carbon film deposition, (b) in-situ sample preparation, (c) in-situ TEM/EELS observation and in-situ heating process.

from 200 °C, which results of poorer mechanical and tribological properties [27]. Carpick et al. used the X-ray photoelectron spectroscopy (XPS) to test the annealed a-C:H film and found the activation energy of C—H sp3 bond is about half of the C—C sp3 bond. The energy of sp2 carbon's clustering and ordering is 10% of the C—H bond [36]. For pure carbon films without hydrogen, Friedmann et al. studied the thermal stability of hydrogen-free, amorphous tetrahedrally coordinated carbon (a-tC) films deposited by pulsed laser deposition (PLD) method with Raman spectroscopy. They found no significant change of Raman spectrum with temperature up to 800 °C [28]. Another study on the post annealing effect on the a-tC film deposited with mass selected ion beam deposition (MSIBD) system was carried out by Kalish et al. They found the correlation between the thermal stability and their initial sp3/sp2 configuration: the carbon film with 60% sp2 fraction started the graphitization at 427 °C while the film with 20% sp2 fraction stayed stable even at 1000 °C [29].

As we can see, most experimental studies on the temperature influence on carbon film are ex-situ experiments, they ether anneal samples from same batch with different temperature then test the annealed ones or heat the same sample with different temperature out of the observation or testing instruments [30–33]. In these situations, the effects from the differences of the same batch samples and the transfer process cannot be ruled out completely, which may have a misleading to the final result. Few in-situ experiments were carried out [7,28,35], but they used in-situ spectroscopy technique, the local information in high spatial resolution is still lacking. A combination of in-situ TEM and EELS study on the carbon film within a wide temperature range can observe and analyze the thermal induced evolution of same carbon film's morphology, atomic structure, electronic structure and chemical composition, which is an ideal solution to solve the problem mentioned above.

In this study, two nanostructured carbon films with similar initial sp2/sp3 ratio were deposited by ion and electron irradiated ECR sputtering respectively. The atomic and electronic structural evolutions in the same areas of these two films were monitored by in-situ TEM and EELS from 25 °C to 1000 °C. We observed significant atomic structure rearrangement and a large increase of sp2/sp3 ratio in the ion irradiated carbon film during the heating process. In the electron irradiated carbon film, the atomic structure rearrangement is mild and its sp2/sp3 ratio was preserved up to 1000 °C. We suggest that the heated argon atoms knocked on and transferred the kinetic energy to the carbon structure, then triggered the carbon sp3-to-sp2 conversion in the ion irradiated sample.

2. Experimental

2.1. Carbon film fabrication

The carbon film was deposited on p-type ⟨1 0 0⟩ Si substrates (20 × 20 mm, 500 μm thick) by an electron cyclotron resonance plasma sputtering system [13–15]. The schematic of the deposition system has been shown in Fig. 1(a). Before deposition, the system was evacuated to 5.0×10^{-5} Pa with mechanical and turbo pumps. Pure argon (99.999%) was injected to the system and maintained the gas pressure at 4.0×10^{-2} Pa. A 2.45 GHz microwave was introduced to the sputtering chamber to generate the Ar plasma through a rectangular waveguide and a fused quartz window. A bias of -500 V was set on the cylindrical carbon target to start the sputtering process. Mirror confinement and divergent magnetic field were introduced with different magnetic coils setting for electron and ion irradiation ECR deposition, respectively. The irradiation energy was set by applying a bias on the substrate. In this study, the energy was set to 20 eV in both electron and ion irradiation to have similar as-deposited sp2 contents of ~68%. The XPS were employed to check if the carbon films were contaminated from the chamber. As shown in Fig. S1, no impurities from the ECR system source or chamber were found.

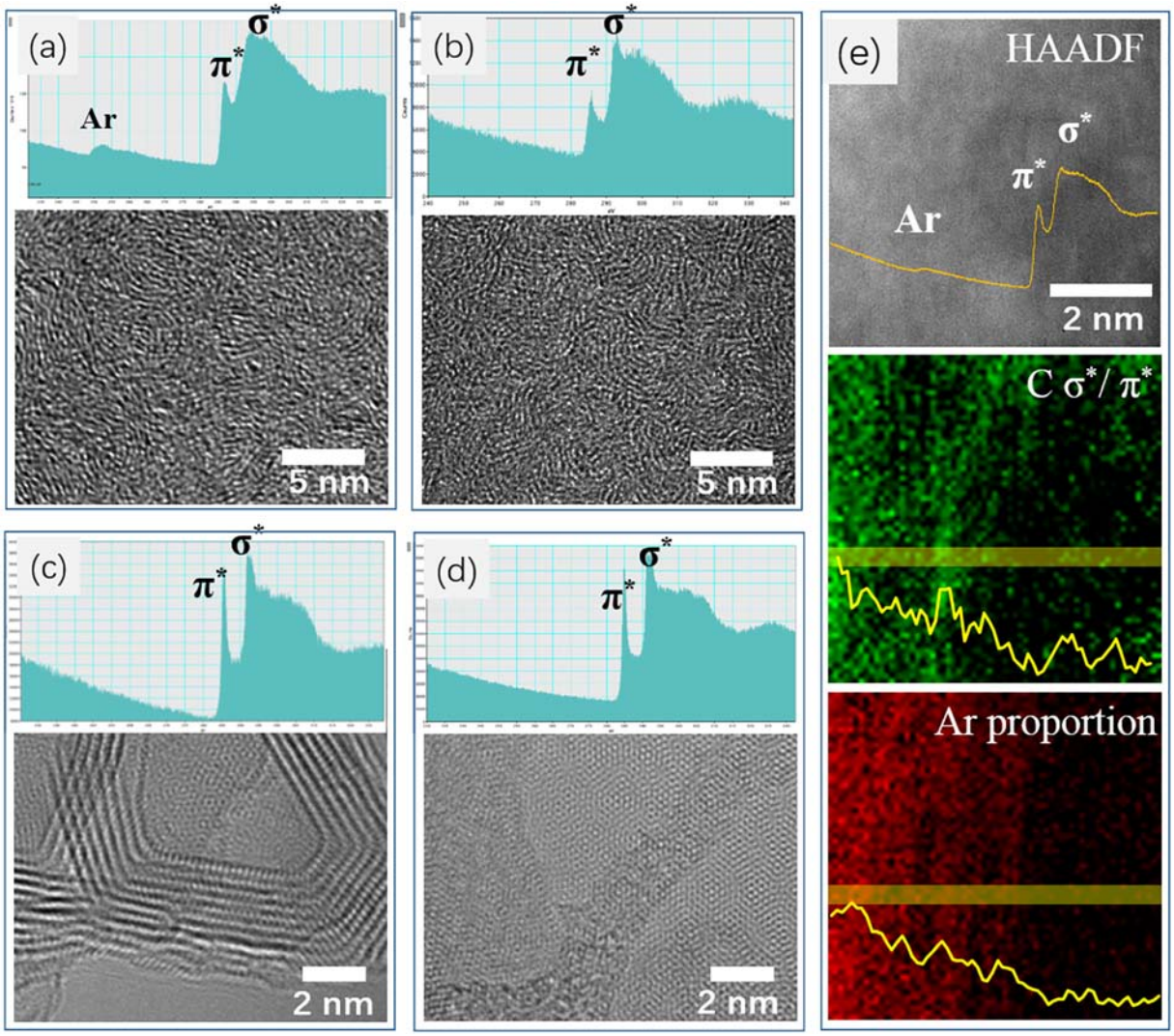

Fig. 2. The as-deposited EELS and TEM images of (a) ion and (b) electron irradiated ECR carbon film. The released large graphene sheets can be occasionally found in both ion and electron irradiation samples, as shown in (c) and (d) respectively. (e) The ion irradiated carbon film's HAADF image (up) and EELS mapping of σ*/π* peak ratio (middle) and Ar L2,3 edge signal (down). The line profiles of σ*/π* peak ratio and Ar L2,3 edge signal are shown in (middle) and (down), respectively.

2.2. Carbon film characterization

The carbon film was released by scratching and transferred on the MEMS heating chips as shown in Fig. 1(b). An aberration-corrected FEI Titan^3 Themis G2 TEM (Electron Microscopy Center, Shenzhen University) equipped with a Gatan Quantum ER/965 EELS detector was employed to perform the TEM imaging and electron energy loss spectroscopy. The configuration of the in-situ experiment has been shown in Fig. 1(c). The TEM was operated at 80 kV accelerate voltage to minimize electron beam damage on the carbon sample. A FEI NanoEx-i/v heating holder with MEMS chips was used to perform the in-situ heating as shown in Fig. 1(c), ion and electron irradiated samples were heated from 25 °C to 1000 °C with steps of 200 °C respectively. Each step was kept for around 30 min for stabilization, TEM imaging and EELS recording. The TEM images were recorded by a Ceta2 camera with an electron dose of ~5×10^5 electron/nm^2. The EELS spectra were obtained by a Gatan Quantum ER/965 detector during scanning over the film. The energy dispersion was set to 0.05 eV/channel, with a 2.5 mm aperture. Each final spectrum was summed up with 20 single 0.5 s-acquired spectra. The EELS collection angle was set to 3.6mrad, which is the magic angle for 80 kV EELS, to minimize the anisotropy effect of carbon crystallite [37,38]. For sp2/sp3 ratio quantification, the background and plural scattering were removed from the carbon K-edges using Digital Micrograph (TM) software. The influence of the electron beam on the carbon film has been tested by performing the continuous electron beam (with the same setting of normal in-situ experiment) irradiation on the samples for 20 min (the total electron dose is larger than the electron dose in the whole in-situ experiment) beam irradiation test are shown in Fig. S2, no significant difference of carbon K-edge and argon L-edge can be distinguished, which proves that in our experimental condition, the damage effect from the electron beam was minimized.

3. Results and discussion

3.1. As-deposited carbon films and Ar trapping location

The as-deposited samples were first characterized by TEM and EELS. As shown in Fig. 2(a) and (b), both ion and electron irradiated samples have the nanocrystallite structures inside the film. No significant difference can be distinguished through the images. In the EELS core loss spectra, the argon signal can only be observed in the ion irradiated sample, indicating the existence of argon trapped inside the film from argon ion irradiation. The EELS C_K edge general shapes of two carbon films are quite different, compare with the ion irradiated carbon film, the electron irradiated sample has a sharper 1s-σ* peak at ~291 eV

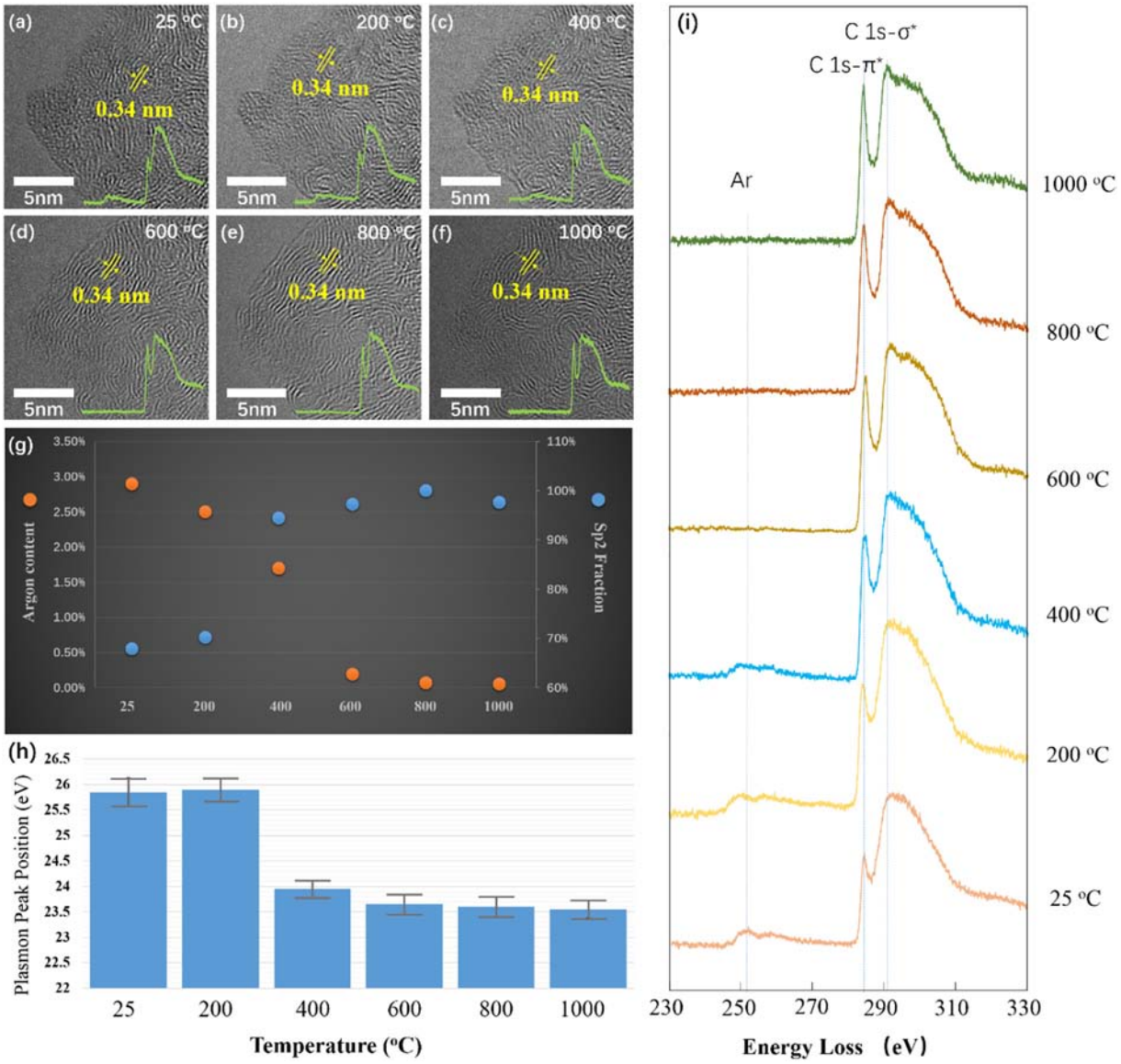

Fig. 3. (a)–(f) The TEM images and corresponding EELS spectra of the ion irradiated carbon film with the temperature from 25 °C to 1000 °C. (g) Sp2 fraction and argon content of ion irradiated carbon film with the temperature from25 °C to 1000 °C. (h) Plasmon peak position as a function of temperature from 25 °C to 1000 °C. (i) EEL spectra of the ion irradiated carbon film with the temperature from 25 °C to 1000 °C.

which is similar to the pure sp2 crystallite and normally considered as a symbol of higher level of ordering or clustering of sp2 bond carbon. Pure sp2 crystallite sheets can be found occasionally in both ion and electron irradiated samples as shown in Fig. 2(c) and (d). There is no argon signal found in the pure sp2 crystallite sheets from ion-irradiation samples, which implies the argon can be only implanted in the small voids in the amorphous carbon. To prove this, an EELS mapping was employed on the ion-irradiated carbon film as shown in Fig. 2(e). From up to down is the HAADF image, the mapping of σ*/π* peak ratio and the argon signal of the ion irradiated carbon film, their corresponding intensity line profiles are shown in the mapping images. Comparing the σ*/π* peak ratio and the argon signal, it is quite clear that the argon tends to be stored in the higher σ*/π* (more amorphous in our case) region.

3.2. Atomic and electronic structural evolution of ion-irradiated carbon film

The in-situ heating experiments of ion-irradiated carbon film from 25 °C to 1000 °C were carried out inside the TEM with a MEMS based heating holder, the TEM images and corresponding EELS of the same area of carbon film with increasing temperature are shown in Fig. 3(a)–(f). From the atomic resolution TEM images, we can see the shape of the film edge is generally preserved even at 1000 °C, however the atomic structure inside the shape changed with increasing temperature: the amorphous carbon transferred to multilayer graphene sheets and small embedded graphene sheets linked together to form bigger multilayer graphene structures (according to the 3.4 nm d-spacing and the layers number is below 10) [39]. This atomic rearrangement started from 200 °C and almost completed at 600 °C. From the corresponding EELS core loss spectra, more details in electronic structure and composition of the carbon film are revealed: first, the argon signal started decreasing from 200 °C and disappeared at 600 °C; second, the relative height of π* peak grew from 200 °C and after 600 °C the peak height stopped growing and maintained the height till 1000 °C. This implies the general electronic structure changing occurred during the heating process; third, the width of the π* peak narrowed slightly and a small σ* peak arise at ~291 eV with the increasing temperature, which normally implies the expansion of sp2 crystallization. Further quantitative core loss EELS analysis of carbon film's sp2/sp3 ratio was carried out by two window method with pure sp2 crystal (multilayer

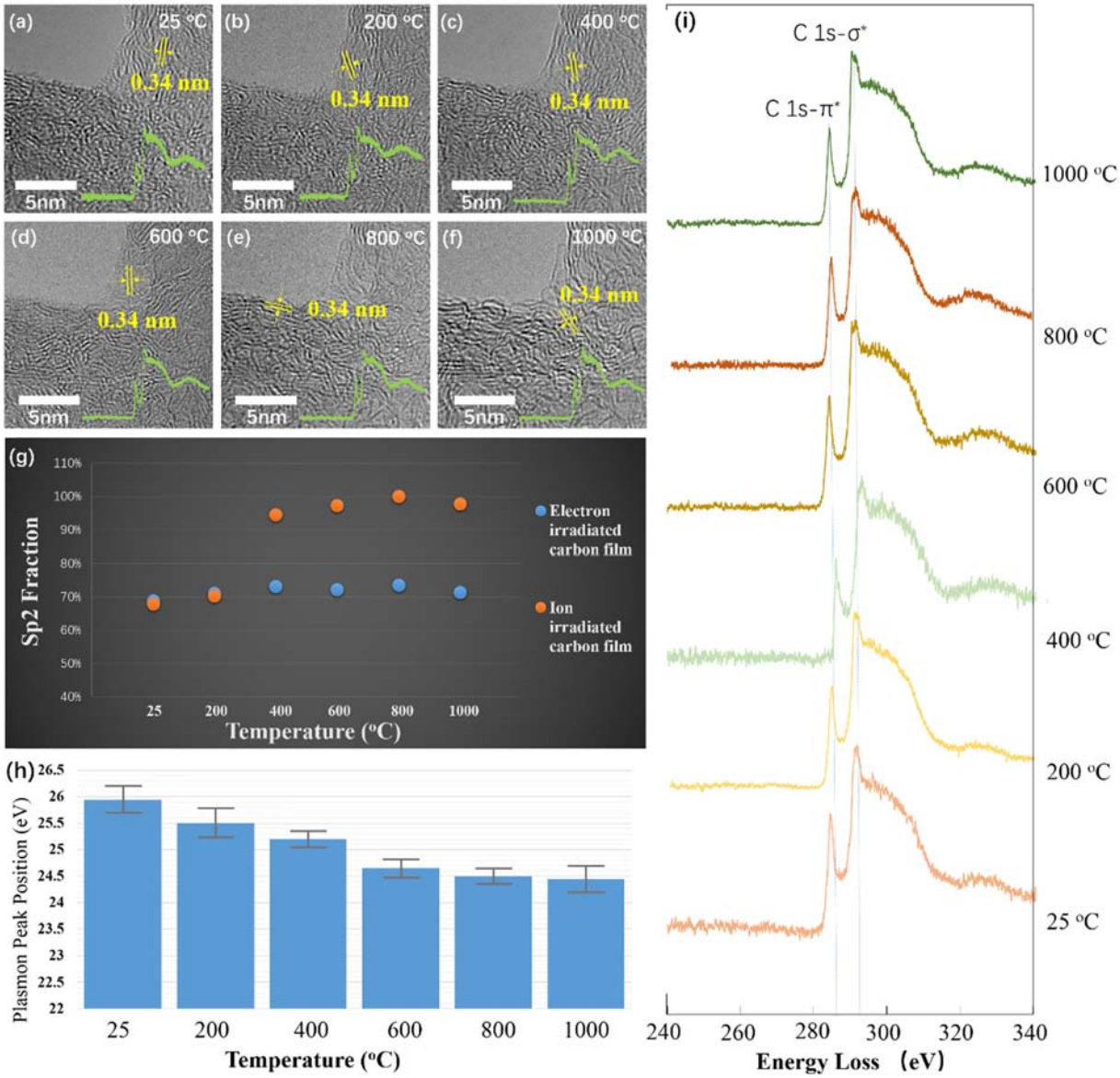

Fig. 4. (a)–(f) The TEM images and corresponding EELS spectra of the electron irradiated carbon film with temperature from 25 °C to 1000 °C. (g) Graph of ion argon concentration and sp2 fraction with temperature from 25 °C to 1000 °C. (h) Plasmon peak position as a function of temperature from RT to 1000 °C. (i) EELS spectra of the electron irradiated carbon film with temperature from 25 °C to 1000 °C.

graphene) as reference. The sp2 content and argon concentration as a function of heating temperature are shown in Fig. 3(g). The sp2 content of the as deposited sample is 67.9%, which remains almost same (70.2%) at 200 °C, then the sp2 content grows rapidly to 94.5% at 400 °C, then grows to almost 100% from 600 °C. With the increasing sp2 content, the argon concentration (2.9% at 25 °C) decreases simultaneously and disappeared completely at 600 °C. The temperature influence can also be observed in low loss EELS spectra. The bulk plasmon energy as a function of temperature is shown in Fig. 3(i). It is clearly showed that the plasmon energy rapidly declined at 400 °C, reflecting a decreasing of the valance electron density (the plasmon energy E_p is directly proportional to valance electron density) which is mainly from the sp3-to-sp2 hybridization conversion as shown in Fig. 3(g). The argon releasing and sp2 carbon clustering also have a relative small effect on the bulk plasmon energy (the former will increase the plasmon energy while the latter decrease it), which should be responsible for the small energy shift at 25–200 °C and 400-600 °C.

3.3. Atomic and electronic structural evolution of electron-irradiated carbon film

The temperature influence on electron irradiated carbon film was also studied by in-situ TEM and EELS. The results are shown in Fig. 4(a)–(f). The experimental procedure was same with experiment on the ion-irradiated sample. From TEM images, we can see the shape of the film doesn't change up to 1000 °C. A slight clustering of sp2 carbon can be observed, but with a lower level compared with the ion irradiated carbon film. Through the corresponding core loss EELS, we can see no significant variation occurs from 25 °C till 1000 °C, very small changes can be found with π* and σ* peak shape, but not as obvious as the changes in ion-irradiated sample. In the quantitative core loss EELS analysis as shown in Fig. 4(g), comparing with the rapid increasing of sp2 content from 68% at 25 °C to the 94% at 400 °C in the ion irradiated carbon film, the sp2 content of the electron irradiated sample almost preserved in the range from 68% to 73% up to 1000 °C, showing very little influence from the increasing temperature. In the low loss EELS as shown in Fig. 4(i), the bulk plasmon energy decreased from ~25.9 eV at

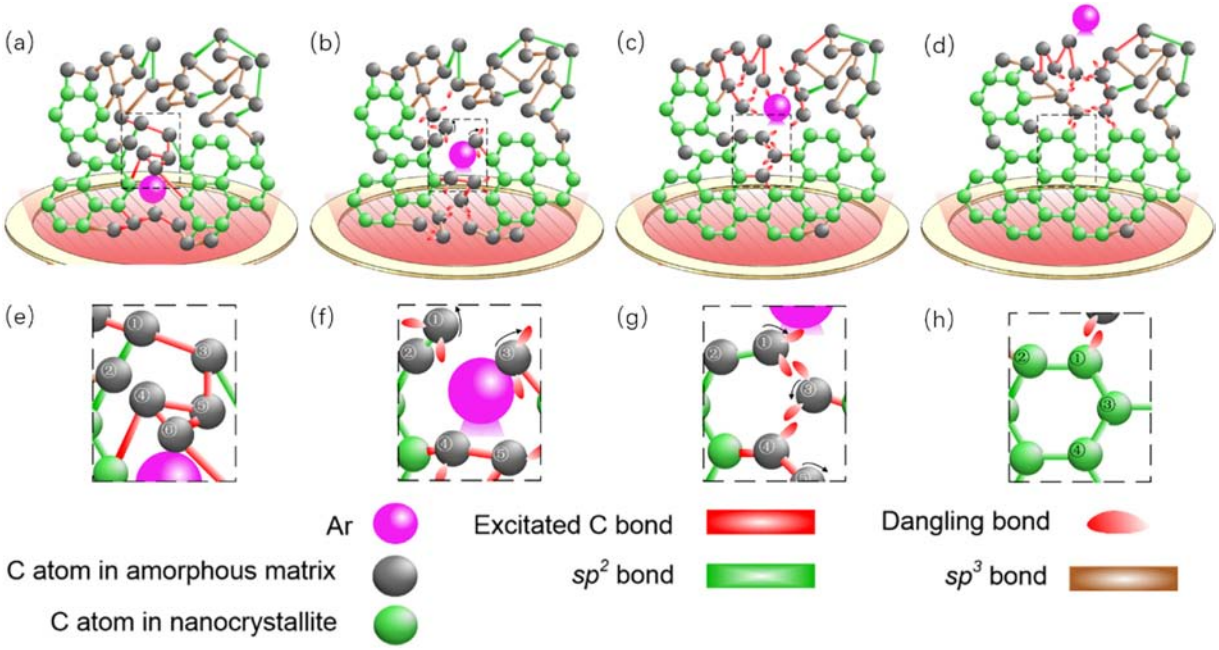

Fig. 5. The schematic of the sp3-sp2 conversion triggered by the heated argon. (a)–(d), the process of argon atom release and the following sp3-sp2 conversion triggered by it. (e)–(f), the corresponding highlights of the argon-carbon interaction.

25 °C to ~24.4 eV at 1000 °C, which is also smaller than the decline happened in ion irradiated carbon film. As shown in core loss EELS, no obvious sp3-to-sp2 conversion occurred, the decreased plasmon energy should be mainly from the clustering of sp2 carbon and the lattice expansion of the carbon film. When the sp2 clusters growing longer, they tend to curl and form small voids which reduce the carbon film's density, therefore lower the bulk plasmon energy. A recent research reported that the crystal lattice of carbon can expand during the heating process [40], this lattice expansion can also lead to the lower film's density and bulk plasmon energy. Another possible factor is the trapped electron emission. In the electron irradiated carbon film, excess electrons are trapped in the embedded graphene edge defects, resulting of a lower work function of the film. So during the heating process, the trapped instable excess electrons may be emitted, which can also reduce the electron density and decrease the bulk plasmon energy peak in low loss EELS.

3.4. Discussion

As shown in Fig. 4(g), the ion and electron irradiated ECR carbon films showed very different performance during the same heating process, the reason behind this needs to be discussed thoroughly. Previous study suggested that the carbon films with different sp2/sp3 hybridization ratio can lead to different thermal stability [29]. As both two samples in our study have very close initial sp2/sp3 ratio, this effect can be excluded. The desorption of chemical or physical adsorbed water can affect the carbon film's electronic structure, but as shown in Fig. S3, the survey EELS shows no oxygen signal in both samples, so the influence of water desorption can be ruled out as well. The doping that widely used as a technique to alter the carbon film's properties can also influence the carbon film's thermal stability: the weak C—H bond is normally considered to be responsible for weakening the carbon film's thermal stability while the nitrogen doping is reported that can change the thermal stability in both ways [7,41,42]. However, all the research studied the influence of the chemical bonding between carbon and doped atoms, the residual inert atoms like argon were neglected. In this study, as shown in Figs. S1 and S3, no chemical bonded doping like hydrogen or nitrogen was applied on the carbon films, the major difference is the argon and the trapped excess electrons which existed in the ion and electron irradiated ECR films respectively. In Fig. 3(g), we can see a clear correlation between the argon concentration and the sp2/sp3 ratio. Based on these observations, we propose a mechanism of the argon's role in the carbon film heating experiment.

The schematics is shown in Fig. 5. We have known that the residual argons were all implanted in the amorphous carbon region from Fig. 2. When the sample was heated as shown in Fig. 5(a), the weak van der Waals bond broke and the heated hot argon atom started to knock on the nearby amorphous carbon structures. When the temperature arrives certain value, in our case above 200 °C, the hot argon breaks the heat excited sp2 and sp3 bonds, produced the dangling bonds (shown in Fig. 5(b)), as the sp2 bond has lower energy, dangling bond tend to form the sp2 bond, which lead to the sp3-to-sp2 conversion and sp2 clustering as shown in Fig. 5(c). This process continues until the argon released from the film. In the electron irradiated sample, without the hot argon's “knock on” effect, the high temperature applied in this study can only overcome the activation energy for clustering of sp2 carbon atoms and is not enough for carbon sp3-to-sp2 conversion. So during the heating process, we can only see the carbon clustering and ordering, the sp2/sp3 hybridization ratio remained till the highest 1000 °C.

Inert ion beam irradiation was successfully introduced to optimize the carbon film's performance ether during the carbon film deposition to assist the film growth or after deposition to induce the carbon film's structure transformation [15,37,43–46]. The ion-carbon interaction during the ion irradiation is well considered and regarded as the reason of the carbon film modification, however very few attention has been drawn on the residual argon inside the film and their effect on the film's properties. Some studies noticed the residence of argon atoms, but their effect was long being neglected due to their low concentration and inert property [45]. As we presented in this paper, the influence of residual argon inside the carbon film can be significant, and the influence of these residual inert atoms in the carbon film should not be ignored in the future studies.

From the in-situ experiment, the atomic and electronic structural evolution of both ion and electron irradiated nanostructured carbon film from 25 °C to 1000 °C were resolved. So how can these evolutions affect the different properties of the carbon films. For tribological property, the ion irradiated carbon film will preserve its original tribological performance in 200 °C, above that it will be more lubricous

due to more sp2 graphene sheet, but its wear life will decrease because of the less content of sp3 contained amorphous carbon which stabilize the carbon film's structure. The electron irradiated carbon film, in the other hand, should show a better tribological thermostability. Due to the stable hybridization ratio, it may maintain its tribological property till 1000 °C. In general, the electron irradiated carbon shows better thermal stability than the ion irradiated one in most properties as the sp3-to-sp2 conversion doesn't occur significantly under 1000 °C. However, for properties like field emission property, the thermal stability of the trapped excess electrons in the electron irradiated carbon film need to be further considered.

4. Conclusion

In summary, the high temperature influence on the ion and electron irradiated nanostructured carbon films were studied by in-situ TEM and EELS from 25 °C to 1000 °C. With the atomic resolution TEM imaging, both ion and electron irradiated carbon films preserved their outer shape even at 1000 °C and the atomic rearrangement was observed in both samples from 200 °C. However, the differences from the two samples were found from the quantitative core loss EELS analysis. The electron irradiated sample preserved its sp2/sp3 ratio even at 1000 °C, while the ion-irradiated sample started the sp3-to-sp2 conversion from 200 °C and completed at 600 °C. The residual argon atoms which only found in the ion-irradiated carbon film effused simultaneously with the carbon sp3-to-sp2 conversion and are considered as the reason of the ion-irradiated carbon film's weaker thermal stability. For the first time, the influence of residual inert argon in the graphene sheets embedded carbon film was reported. When introduce the widely used argon ion irradiation technique, the effect of the implanted residual cannot be neglected, especially when the high thermal stability is required. On the other hand, as no residual atoms implanted, the electron irradiation technique shows its advantage and can be a desirable technique to synthesize or modify high thermal stable carbon film.

Acknowledgement

The authors would like to thank the financial support of National Natural Science Foundation of China (11904235 and 51975383), Shenzhen Fundamental Research Project (JCYJ20160427105015701).

Appendix A. Supplementary data

Supplementary data to this article can be found online at https://doi.org/10.1016/j.apsusc.2019.143831.

References

[1] Y. Gao, T. Cao, F. Cellini, C. Berger, W.A. De Heer, E. Tosatti, E. Riedo, A. Bongiorno, Ultrahard carbon film from epitaxial two-layer graphene, Nat. Nanotechnol. 13 (2018) 133–138, https://doi.org/10.1038/s41565-017-0023-9.
[2] C. Sui, Y. Yang, R.J. Headrick, Z. Pan, J. Wu, J. Zhang, S. Jia, X. Li, W. Gao, O.S. Dewey, C. Wang, X. He, J. Kono, M. Pasquali, J. Lou, Directional sensing based on flexible aligned carbon nanotube film nanocomposites, Nanoscale 10 (2018) 14938–14946, https://doi.org/10.1039/c8nr02137f.
[3] M.L. Geier, J.J. McMorrow, W. Xu, J. Zhu, C.H. Kim, T.J. Marks, M.C. Hersam, Solution-processed carbon nanotube thin-film complementary static random access memory, Nat. Nanotechnol. 10 (2015) 944–948, https://doi.org/10.1038/nnano.2015.197.
[4] Y. Liu, Q. Liu, C. Zhou, C. Lau, X. Cao, F. Wu, Top-contact self-aligned printing for high-performance carbon nanotube thin-film transistors with sub-micron channel length, ACS Nano 11 (2017) 2008–2014, https://doi.org/10.1021/acsnano.6b08185.
[5] Y. Wang, Q. Wei, Z. Yu, H. Long, Z. Deng, Y. Xie, J. Li, C. Te Lin, L. Ma, K. Zhou, Field emission properties of the caterpillar-like structural carbon film grown by magnetic and electric fields coupling HFCVD, Appl. Surf. Sci. 423 (2017) 788–792, https://doi.org/10.1016/j.apsusc.2017.06.240.
[6] W. Zhuang, X. Fan, W. Li, H. Li, L. Zhang, J. Peng, Z. Cai, J. Mo, G. Zhang, M. Zhu, Comparing space adaptability of diamond-like carbon and molybdenum disulfide films toward synergistic lubrication, Carbon 134 (2018) 163–173, https://doi.org/10.1016/j.carbon.2018.03.059.
[7] Y. Zhang, K. Polychronopoulou, M. Humood, A.A. Polycarpou, High temperature nanotribology of ultra-thin hydrogenated amorphous carbon coatings, Carbon 123 (2017) 112–121, https://doi.org/10.1016/j.carbon.2017.07.047.
[8] R.J. Yeo, N. Dwivedi, L. Zhang, Z. Zhang, C.Y.H. Lim, S. Tripathy, C.S. Bhatia, Superior wear resistance and low friction in hybrid ultrathin silicon nitride/carbon films: synergy of the interfacial chemistry and carbon microstructure, Nanoscale 9 (2017) 14937–14951, https://doi.org/10.1039/c7nr03737f.
[9] L. Chen, D. Huang, S. Ren, T. Dong, Y. Chi, G. Chen, Preparation of graphite-like carbon nitride nanoflake film with strong fluorescent and electrochemiluminescent activity, Nanoscale 5 (2013) 225–230, https://doi.org/10.1039/c2nr32248j.
[10] B. Narayanan, S.K.R.S. Sankaranarayanan, G. Kamath, O.L. Eryilmaz, Y. Liao, A. Erdemir, G. Ramirez, Carbon-based tribofilms from lubricating oils, Nature 536 (2016) 67–71, https://doi.org/10.1038/nature18948.
[11] S. Hirono, S. Umemura, M. Tomita, R. Kaneko, Superhard conductive carbon nanocrystallite films, Appl. Phys. Lett. 80 (2002) 425–427, https://doi.org/10.1063/1.1435402.
[12] L.H. Chou, W.T. Hsieh, Effects of argon ion bombardment on the microstructures and electrical conductivities of hydrogenated amorphous carbon films prepared by plasma-enhanced chemical vapor deposition, J. Appl. Phys. 75 (1994) 2257–2263, https://doi.org/10.1063/1.356289.
[13] C. Wang, D. Diao, Cross-linked graphene layer embedded carbon fi lm prepared using electron irradiation in ECR plasma sputtering, Surf. Coat. Technol. 206 (2011) 1899–1904, https://doi.org/10.1016/j.surfcoat.2011.08.009.
[14] C. Wang, D. Diao, X. Fan, C. Chen, Graphene sheets embedded carbon film prepared by electron irradiation in electron cyclotron resonance plasma, Appl. Phys. Lett. 100 (2012) 213909, , https://doi.org/10.1063/1.4727894.
[15] X. Fan, D. Diao, Ion excitation and etching effects on top-surface properties of sp2nanocrystallited carbon films, Appl. Surf. Sci. 462 (2018) 669–677, https://doi.org/10.1016/j.apsusc.2018.08.148.
[16] L. Huang, Y. Cao, D. Diao, Nanosized graphene sheets induced high electrochemical activity in pure carbon film, Electrochim. Acta 262 (2018) 173–181, https://doi.org/10.1016/j.electacta.2018.01.027.
[17] W. Zhang, D. Diao, K. Sun, X. Fan, P. Wang, Study on friction-electrification coupling in sliding-mode triboelectric nanogenerator, Nano Energy 48 (2018) 456–463, https://doi.org/10.1016/j.nanoen.2018.04.007.
[18] P. Xue, L. Yang, D. Diao, Nanocrystalline/amorphous biphase enhanced mechanical properties in multilayer carbon films, Surf. Coat. Technol. 334 (2018) 1–6, https://doi.org/10.1016/j.surfcoat.2017.10.061.
[19] K. Sun, D. Diao, L. Yang, W. Zhang, X. Fan, Nanosized graphene sheets enhanced electron field emission behavior in pure carbon film, Thin Solid Films 664 (2018) 124–129, https://doi.org/10.1016/j.tsf.2018.08.024.
[20] W. Chen, X. Zhang, D. Diao, Low-energy electron excitation effect on formation of graphene nanocrystallites during carbon film growth process, Appl. Phys. Lett. 111 (2017), https://doi.org/10.1063/1.4990117.
[21] C. Wang, D. Diao, Self-magnetism induced large magnetoresistance at room temperature region in graphene nanocrystallited carbon film, Carbon 112 (2017) 162–168, https://doi.org/10.1016/j.carbon.2016.11.009.
[22] C. Chen, X. Fan, D. Diao, Low-energy electron irradiation induced top-surface nanocrystallization of amorphous carbon film, Appl. Surf. Sci. 384 (2016) 341–347, https://doi.org/10.1016/j.apsusc.2016.05.042.
[23] L. Yang, G. Hu, D. Zhang, D. Diao, Nanosized graphene sheets enhanced photoelectric behavior of carbon film on p-silicon substrate, Appl. Phys. Lett. 109 (2016) 031910, , https://doi.org/10.1063/1.4959563.
[24] X. Zhang, C. Wang, C.Q. Sun, D. Diao, Magnetism induced by excess electrons trapped at diamagnetic edge-quantum well in multi-layer graphene, Appl. Phys. Lett. 105 (2014) 1–5, https://doi.org/10.1063/1.4891558.
[25] C. Wang, X. Zhang, D. Diao, Nanosized graphene crystallite induced strong magnetism in pure carbon films, Nanoscale 7 (2015) 4475–4481, https://doi.org/10.1039/c4nr06711h.
[26] D.R. Tallant, J.E. Parmeter, M.P. Siegal, R.L. Simpson, The thermal stability of diamond-like carbon, Diam. Relat. Mater. 4 (1995) 191–199, https://doi.org/10.1016/0925-9635(94)00243-6.
[27] H. Li, T. Xu, C. Wang, J. Chen, H. Zhou, H. Liu, Annealing effect on the structure, mechanical and tribological properties of hydrogenated diamond-like carbon films, Thin Solid Films 515 (2006) 2153–2160, https://doi.org/10.1016/j.tsf.2006.04.018.
[28] T.A. Friedmann, K.F. McCarty, J.C. Barbour, M.P. Siegal, D.C. Dibble, Thermal stability of amorphous carbon films grown by pulsed laser deposition, Appl. Phys. Lett. 68 (1996) 1643–1645, https://doi.org/10.1063/1.115891.
[29] R. Kalish, Y. Lifshitz, K. Nugent, S. Prawer, Thermal stability and relaxation in diamond-like-carbon. A Raman study of films with different sp3 fractions (ta-C to a-C), Appl. Phys. Lett. 74 (1999) 2936–2938, https://doi.org/10.1063/1.123971.
[30] O.R. Monteiro, J.W. Ager, D.H. Lee, R.Y. Lo, K.C. Walter, M. Nastasi, Annealing of nonhydrogenated amorphous carbon films prepared by filtered cathodic arc deposition, J. Appl. Phys. 88 (2000) 2395–2399, https://doi.org/10.1063/1.1288221.
[31] C. Chen, D. Diao, Tribological thermostability of carbon film with vertically aligned graphene sheets, Tribol. Lett. 50 (2013) 305–311, https://doi.org/10.1007/s11249-013-0129-7.
[32] S. Takabayashi, K. Okamoto, T. Nakatani, Influence of post-annealing on a diamondlike carbon film analyzed by Raman spectroscopy, Surf. Interface Anal. 50 (2018) 441–447, https://doi.org/10.1002/sia.6387.
[33] N. Khamnualthong, K. Siangchaew, P. Limsuwan, Influence of thermal heating on diamond-like carbon film properties prepared byfiltered cathodic arc, Thin Solid Films 544 (2013) 477–481, https://doi.org/10.1016/j.tsf.2013.02.074.
[34] D.S. Grierson, A.V. Sumant, A.R. Konicek, T.A. Friedmann, J.P. Sullivan, R.W. Carpick, Thermal stability and rehybridization of carbon bonding in

tetrahedral amorphous carbon, J. Appl. Phys. 107 (2010) 033523, , https://doi.org/10.1063/1.3284087.
[35] M. Rouhani, F. Chau-Nan Hong, Y.R. Jeng, In-situ thermal stability analysis of amorphous carbon films with different sp3content, Carbon 130 (2018) 401–409, https://doi.org/10.1016/j.carbon.2018.01.034.
[36] F. Mangolini, F. Rose, J. Hilbert, R.W. Carpick, Thermally induced evolution of hydrogenated amorphous carbon, Appl. Phys. Lett. 103 (2013) 161605, , https://doi.org/10.1063/1.4826100.
[37] X. Zhang, R. Schneider, E. Müller, D. Gerthsen, Practical aspects of the quantification of sp2-hybridized carbon atoms in diamond-like carbon by electron energy loss spectroscopy, Carbon 102 (2016) 198–207, https://doi.org/10.1016/j.carbon.2016.02.020.
[38] J. Yuan, L.M. Brown, Investigation of atomic structures of diamond-like amorphous carbon by electron energy loss spectroscopy, Micron 31 (2000) 515–525, https://doi.org/10.1016/S0968-4328(99)00132-8.
[39] A. Bianco, H.M. Cheng, T. Enoki, Y. Gogotsi, R.H. Hurt, N. Koratkar, T. Kyotani, M. Monthioux, C.R. Park, J.M.D. Tascon, J. Zhang, All in the graphene family - a recommended nomenclature for two-dimensional carbon materials, Carbon 65 (2013) 1–6, https://doi.org/10.1016/j.carbon.2013.08.038.
[40] M. Hayashida, K. Cui, M. Malac, R. Egerton, Ultramicroscopy thermal expansion coefficient measurement from electron diffraction of amorphous films in a TEM, Ultramicroscopy 188 (2018) 8–12.
[41] O. Cometto, C.A. Dennett, S.H. Tsang, M.P. Short, E.H.T. Teo, A thermal study of amorphous and textured carbon and carbon nitride thin films via transient grating spectroscopy, Carbon 130 (2018) 355–361, https://doi.org/10.1016/j.carbon.2018.01.025.
[42] H.L. Bai, E.Y. Jiang, Improvement of the thermal stability of amorphous carbon films by incorporation of nitrogen, Thin Solid Films 353 (1999) 157–165, https://doi.org/10.1016/S0040-6090(99)00421-6.
[43] T. Yajima, S. Umemura, S. Hirono, A. Imoto, R. Kaneko, Tribological characteristics of highly wear-durable ECR-sputtered carbon film, Surf. Coat. Technol. 169–170 (2003) 274–276, https://doi.org/10.1016/S0257-8972(03)00048-3.
[44] J. Xie, K. Komvopoulos, The effect of argon ion irradiation on the thickness and structure of ultrathin amorphous carbon films, J. Appl. Phys. 119 (2016) 095304, , https://doi.org/10.1063/1.4942440.
[45] S.S. Tinchev, Surface modification of diamond-like carbon films to graphene under low energy ion beam irradiation, Appl. Surf. Sci. 258 (2012) 2931–2934, https://doi.org/10.1016/j.apsusc.2011.11.009.
[46] D.H. Kim, C.D. Kim, H.R. Lee, Effects of the ion irradiation of screen-printed carbon nanotubes for use in field emission display applications, Carbon 42 (2004) 1807–1812, https://doi.org/10.1016/j.carbon.2004.03.015.